

---

*This copy is for your personal, non-commercial use only.*

---

**If you wish to distribute this article to others**, you can order high-quality copies for your colleagues, clients, or customers by [clicking here](#).

**Permission to republish or repurpose articles or portions of articles** can be obtained by following the guidelines [here](#).

**The following resources related to this article are available online at [www.sciencemag.org](http://www.sciencemag.org) (this information is current as of April 28, 2014 ):**

**Updated information and services**, including high-resolution figures, can be found in the online version of this article at:

<http://www.sciencemag.org/content/343/6168/281.full.html>

**Supporting Online Material** can be found at:

<http://www.sciencemag.org/content/suppl/2014/01/15/343.6168.281.DC1.html>

This article **cites 32 articles**, 2 of which can be accessed free:

<http://www.sciencemag.org/content/343/6168/281.full.html#ref-list-1>

This article appears in the following **subject collections**:

Materials Science

[http://www.sciencemag.org/cgi/collection/mat\\_sci](http://www.sciencemag.org/cgi/collection/mat_sci)

# Atomic-Scale Variability and Control of III-V Nanowire Growth Kinetics

Y.-C. Chou,<sup>1,2</sup> K. Hillerich,<sup>3</sup> J. Tersoff,<sup>4</sup> M. C. Reuter,<sup>4</sup> K. A. Dick,<sup>3,5</sup> F. M. Ross<sup>4\*</sup>

In the growth of nanoscale device structures, the ultimate goal is atomic-level precision. By growing III-V nanowires in a transmission electron microscope, we measured the local kinetics in situ as each atomic plane was added at the catalyst-nanowire growth interface by the vapor-liquid-solid process. During growth of gallium phosphide nanowires at typical V/III ratios, we found surprising fluctuations in growth rate, even under steady growth conditions. We correlated these fluctuations with the formation of twin defects in the nanowire, and found that these variations can be suppressed by switching to growth conditions with a low V/III ratio. We derive a growth model showing that this unexpected variation in local growth kinetics reflects the very different supply pathways of the V and III species. The model explains under which conditions the growth rate can be controlled precisely at the atomic level.

The self-assembly of III-V semiconductors into nanowires via a catalytic particle provides rich opportunities for the formation of structures that are difficult to grow by more conventional techniques: heterostructures composed of highly mismatched materials (1, 2), metastable crystal structures (3), and new configurations such as nanowires with regularly arranged defects (4, 5). Precise control over this vapor-liquid-solid growth process, which takes place bilayer-by-bilayer at the catalyst-nanowire (111) interface (6, 7), is key to the formation of such structures and their development for new electronic and optical applications. Variability in the growth process can complicate the formation of precisely controlled individual structures or arrays of identical structures, but may also provide new pathways for understanding growth and developing new crystal configurations.

We used in situ transmission electron microscopy to provide a direct view of the addition of each atomic bilayer to Au-catalyzed GaP nanowires. Under typical growth conditions, where P is supplied in excess, we found marked changes in growth rate from one atomic layer to the next. The observed variability was much greater than expected from nucleation statistics (8) and was found to be correlated with the formation of defects in the nanowire. The variability can be suppressed by reducing the P supply relative to Ga. This dependence on growth conditions can be understood via a simple model as resulting from the very different transport mechanisms for the two species.

Nanowire growth was carried out in an ultrahigh-vacuum transmission electron microscope (UHV TEM) capable of flowing reactive gases over a heated sample (9). III-V growth has not been

widely studied in the TEM (10, 11) because of the complications involved with handling the necessary precursor gases. However, by flowing trimethylgallium (TMGa) and phosphine (PH<sub>3</sub>) at 10<sup>-5</sup> torr over samples heated to ~440°C, we were able to grow GaP nanowires from Au at rates of 0.1 to 3 nm min<sup>-1</sup>. Because these rates are low, we used samples on which nanowire “stubs” ~1 μm in length and 30 to 50 nm in diameter had been grown ex situ from Au aerosol particles

(12), and observed the continued growth at the tips. Movies of growth were recorded using dark-field imaging conditions. We identified the instant at which each atomic layer adds to the nanowire by measuring the configuration of the catalyst-nanowire interface: Each change in the geometry at the trijunction indicates the moment at which a bilayer adds to the nanowire (11). Simultaneously, changes in image contrast indicate the formation of twin defects in the nanowire (see supplementary text). The observations therefore clarify the relationship among layer-by-layer growth kinetics, nanowire structure, pressure, and temperature. We quantified GaP nanowire growth for temperatures of 400° to 440°C. This temperature is within the range used in conventional metal-organic chemical vapor deposition (MOCVD) of GaP nanowires (13). The TMGa pressure ranged from 10<sup>-8</sup> to 10<sup>-6</sup> torr; the PH<sub>3</sub> pressure was 10<sup>-7</sup> to 10<sup>-5</sup> torr. MOCVD growth of GaP is usually carried out in the presence of H<sub>2</sub> carrier gas and with V/III ratios typically 500 or greater (13–15). In situ, there was no H<sub>2</sub> but our V/III ratios ranged from close to this value (100 to 300, referred to as “high”) to much smaller values (down to ~10). The growth rate examined here, 0.1 to 3 nm min<sup>-1</sup>, is lower than for conventional MOCVD

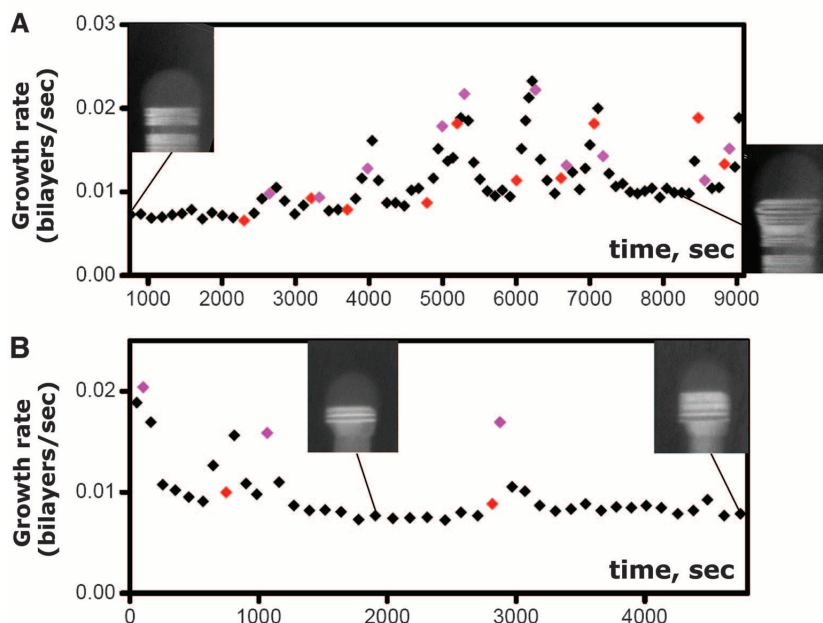


**Fig. 1. Growth kinetics of GaP nanowires under conditions of high V/III ratio.** The instantaneous growth rate is calculated from the interval between the addition of each bilayer. Inset are images of the nanowires at the times indicated. Imaging is in the  $\langle 110 \rangle$  zone axis so that twin contrast is visible. The two twin variants appear as bright and dark bands in the image. Bilayers that were added with a twin orientation are indicated by colored data points. Red points are transitions from the bright to dark twin variant; purple points are transitions from dark to bright. (A) GaP nanowire (diameter 40 nm) showing frequent twin planes, one every 5 to 10 nm. The growth rate fluctuates by a factor of almost 3. During growth the temperature was 440°C, PH<sub>3</sub> pressure varied between  $8 \times 10^{-6}$  and  $1 \times 10^{-5}$  torr, and TMGa pressure varied between  $4 \times 10^{-8}$  and  $8 \times 10^{-8}$  torr. Time is given in seconds since gas exposure began. (B) GaP nanowire (diameter 28 nm) showing increases in growth rate by a factor of 2 associated with the presence of more widely spaced twin pairs. Growth took place at 440°C with PH<sub>3</sub> =  $1.0 \times 10^{-5}$  torr and TMGa =  $5 \times 10^{-8}$  torr. Time is given in seconds since imaging began.

<sup>1</sup>Center for Functional Nanomaterials, Brookhaven National Laboratory, 735 Brookhaven Avenue, Upton, NY 11973, USA.

<sup>2</sup>Department of Electrophysics, National Chiao Tung University, 1001 University Road, Hsinchu City, Taiwan 300, R.O.C. <sup>3</sup>Solid State Physics, Lund University, Box 118, S-221 00 Lund, Sweden. <sup>4</sup>IBM Research Division, T. J. Watson Research Center, Yorktown Heights, NY 10598, USA. <sup>5</sup>Polymer & Materials Chemistry, Lund University, Box 124, S-221 00 Lund, Sweden.

\*Corresponding author. E-mail: fmross@us.ibm.com

but is at the low end of the range for molecular beam epitaxy of GaP (16–19).

Figure 1 and movies S1 and S2 show examples of nanowire growth kinetics measured during GaP growth at 440°C with typical high V/III ratios: TMGa =  $5 \times 10^{-8}$  to  $10 \times 10^{-8}$  torr, PH<sub>3</sub> =  $1.0 \times 10^{-5}$  torr, and V/III ratio = 100 to 200. Growth under these conditions produced nanowires with twinned zinc blende structure, as expected from ex situ growth (15, 20, 21). The graphs show the instantaneous growth rate, calculated from the time interval between addition of successive bilayers to the nanowire. The most striking feature of the data is that GaP nanowires do not grow at a uniform rate, even when the source gas pressures remain constant. At intervals the growth rate increases over a clear baseline rate by as much as a factor of 3 to 4, with the accelerated growth persisting for several bilayers. Moreover, the accelerated growth periods are generally correlated with the appearance of planar defects in the nanowire. These defects may be single twin planes or a closely spaced pair of twin planes. The time at which each defect plane forms is estimated from the image contrast (see supplementary text) and indicated in Fig. 1.

To determine the growth kinetics as a function of pressure, we varied the pressures of TMGa and PH<sub>3</sub> individually while still maintaining a high V/III ratio. The results show no strong dependence of growth rate on PH<sub>3</sub>. This is unsurprising because group V is supplied in excess, as in conventional MOCVD. The growth rate also shows no strong dependence on TMGa pressure (fig. S2), although this was hard to quantify because of the fluctuations.

When we reduced the V/III ratio below ~100, we found radically different growth kinetics. GaP growth with a V/III ratio of 20 to 60 took place with a large and hence Ga-rich droplet (Fig. 2). The addition of bilayers occurred at remarkably regular intervals (Fig. 2, A and B). The lower V/III ratios produced relatively fewer twins than were seen in the high-V/III regime, with only one occurrence in Fig. 2. Examining a broader set of data that includes several twin defects, we consistently find no measurable change in growth rate when a twin defect forms. Furthermore, the growth rate also appears insensitive to the TMGa pressure. This is shown in Fig. 2C, where varying TMGa pressure by a factor of 4 does not affect the growth rate measurably. Instead, the key parameter determining growth rate in this regime is the PH<sub>3</sub> pressure. In Fig. 3, we show that the growth rate is directly proportional to the PH<sub>3</sub> pressure. PH<sub>3</sub>-limited regimes are known from ex situ studies (22).

The local measurements therefore demonstrate two different regimes: (i) at low V/III ratios, a growth rate proportional to PH<sub>3</sub> but with no dependence on TMGa or on crystal defects; and (ii) at high V/III ratios (above ~60 to 100 at the temperature used here), a rate insensitive to PH<sub>3</sub> but with strong local variability that correlates with the formation of twins in the structure.

To derive a compact model that can provide an overview of growth under a broad set of conditions, we neglect discrete aspects of growth such as the nucleation event for each layer (5, 8, 23) and the changing morphology at the growth interface (11, 24). Instead we focus on the well-known differences in transport mechanisms for group III and V atoms (25, 26). A brief outline is given here, with the full derivation and a discussion of nucleation and growth rate in the supplementary text. For simplicity, we consider the limit of fast diffusion of Ga along the surface and into the catalyst, and negligible surface diffusion of P due to its rapid evaporation. As discussed below, the key qualitative conclusions are expected to hold even under more realistic assumptions and should be equally relevant to GaAs and similar III-V nanowire systems. We take the growth rate as proportional to the supersaturation in the catalyst relative to the crystal. Because P diffusion is negligible, the supply of P to the catalyst is proportional to the PH<sub>3</sub> pressure,  $p_V$ , and the catalyst loses excess P by evaporation as well as incorporation into the crystal. In contrast, although the supply of Ga to the surface is proportional to the TMGa pressure  $p_{III}$ , much of this Ga reacts with P on the surface. As a result, the surface acts as a reservoir at chemical potential  $\mu_{Ga} = kT \ln(\alpha p_{III}/p_V)$ , where  $\alpha$  is a surface rate constant (see supplementary text). Thus, the effective Ga supply reflects the V/III

ratio rather than the TMGa pressure. We then calculate the growth rate, finding

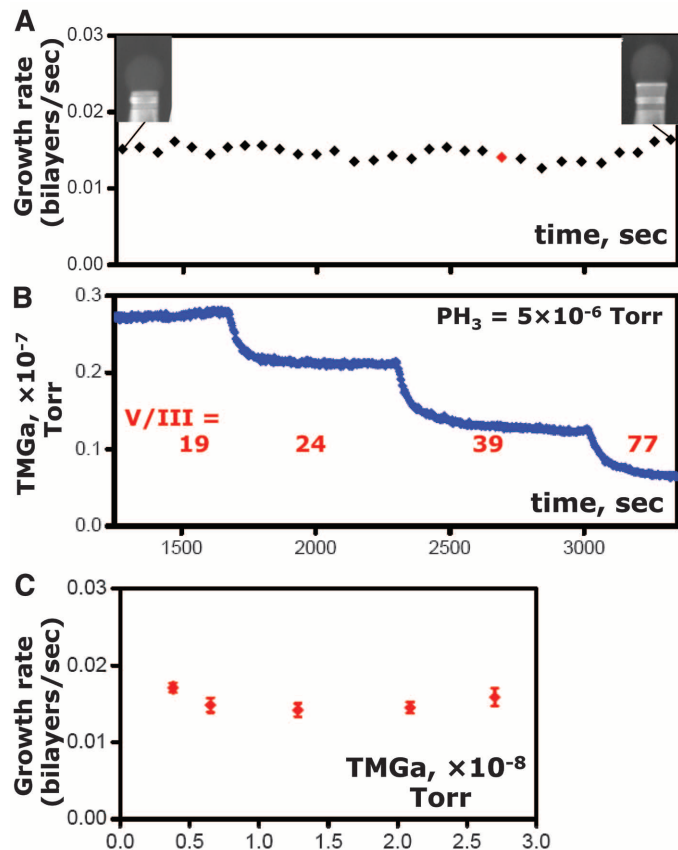
$$v = v_0 \left[ \ln \left( \beta p_V - \frac{v}{v_0} \right) - \ln(\beta p_V) + \ln(\gamma p_{III}) - \frac{\mu_x}{kT} \right] \quad (1)$$

where  $v$  is the growth velocity,  $p_{III}$  and  $p_V$  are the pressures of Ga and P precursors, and  $\mu_x$  is the chemical potential of the nanowire (per two-atom unit, up to an additive constant). The temperature-dependent parameters  $v_0$ ,  $\beta$ , and  $\gamma$  are not known, but we can already see one important point: The growth rate does not depend on the TMGa pressure and nanowire properties independently, but only in the specific combination  $\ln(\gamma p_{III}) - \mu_x/kT$ . Thus, a regime that is insensitive to one of these terms should also be insensitive to the other.

We can quickly see the essentials of the growth behavior by solving Eq. 1 and plotting  $v/v_0$  versus  $\beta p_V$  and  $\ln(\gamma p_{III}) - \mu_x/kT$ . Figure 4 shows qualitatively distinct regimes depending on the gas pressures.

For high group V flux, the growth becomes independent (27) of  $p_V$ . This agrees with the experimental observation that in the high-V/III regime, the GaP growth rate is independent of PH<sub>3</sub> pressure. Instead, the growth rate depends linearly on  $\ln(p_{III}) - \mu_x/kT$  (upper part of Fig. 4).

**Fig. 2. Growth kinetics of a GaP nanowire (diameter 34 nm) under conditions of lower V/III ratio.** Growth took place at 435°C with steady PH<sub>3</sub> =  $5 \times 10^{-6}$  torr and varying TMGa. (A) Instantaneous growth rate, with inset images showing the nanowire structure. The wire has a few twins, about one every 20 to 30 nm. During this experiment only one twin defect forms, and it has no effect on the growth rate. Time is given in seconds since imaging began. (B) TMGa pressure, as measured by mass spectrometer during growth. The V/III ratio is indicated. The TMGa pressure varies by a factor of 4 without measurably affecting the growth rate in (A). (C) Average growth rate as a function of TMGa pressure. The values shown were obtained from the data in (A) and other measurements on the same nanowire at a higher TMGa pressure. Error bars denote SD of the measurements of instantaneous growth rate at each TMGa pressure.



The first term suggests a weak dependence on TMGa pressure in the model; the second term leads to a dependence of growth rate on crystal defects.

In general, any defect or change in local crystal structure will alter the nanowire chemical po-

tential  $\mu_x$ , as will other factors such as any change in diameter, any change in sidewall surface energy, or any change in the angle the sidewalls make with the growth direction. This latter effect arises because of changes in the capillary forces applied by the droplet and the sidewall (28) (supplemen-

tary text). Ex situ observations (15) show that untwinned GaP nanowires grow with {211} sidewalls parallel to the growth direction, and that twins are associated with changes in both nanowire cross-sectional shape and sidewall structure inclination (15). In particular, after a twin, the nanowire grows for a certain length with inclined {111} sidewalls (15, 29). It is difficult to disentangle the effects on  $\mu_x$  of all the changes that occur upon twinning, and indeed our model does not address which feature of the defective crystal changes  $\mu_x$  and hence the growth rate. However, the data in Figs. 1 and 2 do provide some clues. An obvious possibility would be the twin plane itself. However, because the growth rate enhancement persists for several layers, it is unlikely to be an effect of the buried twin plane alone. Indeed, the data in Fig. 1A hint that when there is a pair of twin planes, the first twin is associated with an increasing growth rate, whereas after the second twin plane the growth rate decreases back to the baseline. In (15), when a pair of twins occurs, sidewalls with the opposite inclination form after the second twin, returning the cross section to its original shape. We therefore speculate that upon twinning,  $\mu_x$  and hence the growth rate may be dominated by changes in sidewall energy and/or inclination angle. (We have not confirmed the cross section or inclined facets in our experiments because of the limited resolution of the in situ imaging.)

For high group III flux, the model gives a growth rate that is linear in  $p_V$ . This low-V/III regime is seen at the lower right corner of Fig. 4. The linearity holds as long as  $p_V$  is much greater than the evaporation rate. Most important, in this high  $p_{III}$  pressure limit, the growth rate becomes independent of both  $p_{III}$  and crystal defects or morphological changes. These predictions match well with the observations in Figs. 2 and 3. In this low-V/III regime, the surface is acting as a reservoir of Ga at high chemical potential, with which the catalyst is near equilibrium. Thus, any P arriving at the catalyst is efficiently captured and the growth rate is determined by direct impingement of P atoms, and is therefore insensitive to other factors. The growth rate in this regime would remain linear in  $p_V$  and insensitive to defects even if we included an atomistic nucleation process in the model (see supplementary text).

Although the model is highly simplified, its most important conclusions remain valid under more realistic assumptions and are equally applicable to other III-V nanowire systems. The key requirements to explain the qualitative behavior are only the standard and well-supported assumptions [e.g., (24–26)] that group V diffusion is unimportant relative to direct impingement and evaporation, whereas group III comes primarily from rapid diffusion over a relatively large area.

A third distinct regime is visible at the far left of Fig. 4: If the pressures become too low, the velocity becomes negative as the wire decomposes. However, even our low-pressure experimental conditions appear far from this regime, as evidenced by Fig. 3C.

**Fig. 3. Effect of group V pressure on nanowire growth kinetics.**

(A) Growth kinetics for the same GaP nanowire shown in Fig. 2, but now with varying  $\text{PH}_3$  and steady  $\text{TMGa} = 2.7 \times 10^{-7}$  torr. Inset images show the nanowire structure. One twin forms during the experiment and does not affect the growth rate. Time is given in seconds since imaging began. (B)  $\text{PH}_3$  pressure as measured by mass spectrometer during growth. The V/III ratio is indicated. Note the strong correlation of the growth rate in (A) with  $\text{PH}_3$  pressure. (C) Average growth rate as a function of  $\text{PH}_3$  pressure. Error bars denote SD of the measurements of instantaneous growth rate at each  $\text{PH}_3$  pressure. The dotted line indicates that the growth rate is proportional to the  $\text{PH}_3$  pressure until the  $\text{PH}_3$  pressure rises to values where presumably it is no longer small relative to the TMGa pressure.

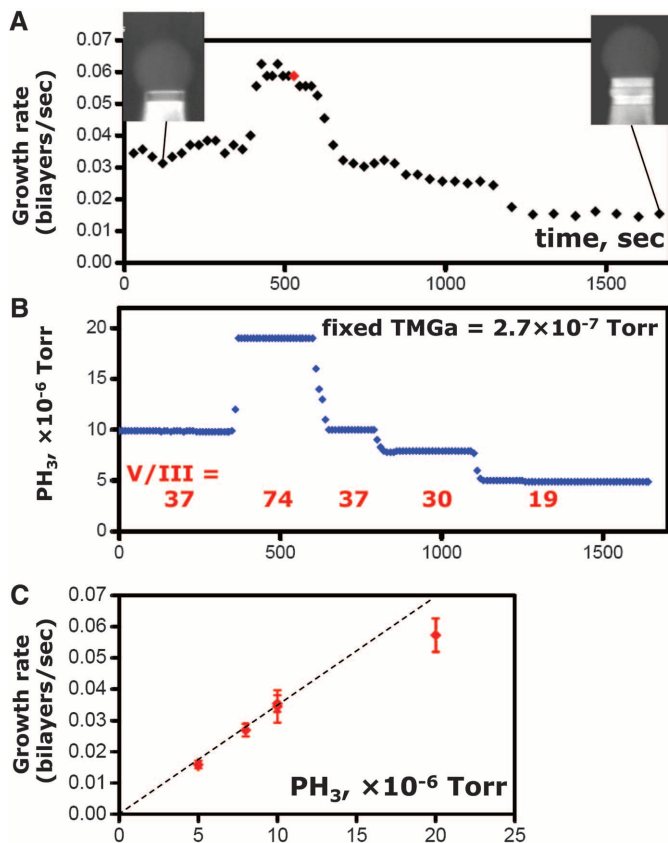
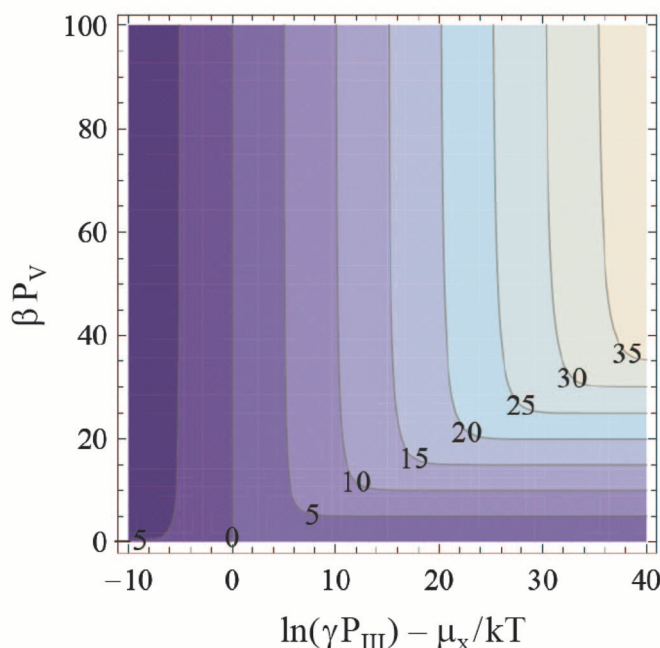


**Fig. 4. Dependence of nanowire growth velocity on gas pressures and nanowire chemical potential  $\mu_x$ , from Eq. 1.** Note the linear scale for group V pressure  $p_V$  and logarithmic scale for group III pressure  $p_{III}$ . Contours of constant velocity are labeled, with velocity increasing from lower left to upper right. In the upper region, corresponding to high V/III ratios, the growth rate becomes independent of  $p_V$  and varies logarithmically with  $p_{III}$  and linearly with  $\mu_x$ . At lower right, corresponding to low V/III ratios, the growth rate becomes independent of  $p_{III}$  and  $\mu_x$  and varies linearly with  $p_V$ .



The relationship between local growth kinetics and atomic structure, obtained through in situ measurements during GaP nanowire growth over a range of parameters, provides insights into understanding the growth mechanism and the requirements for the most precise control over growth. A high V/III ratio is commonly used, but we find local variations in growth rate by as much as a factor of 4. These variations appear to be correlated with changes in the crystal structure associated with twin defects, and we suggest that changes in sidewall configuration are an important factor. The key implication is that the growth rate is very sensitive to perturbations, and such sensitivity must be suppressed to achieve the ultimate control over structure. We find that this sensitivity is absent when growing at low V/III ratios, creating a highly regular regime that may be optimal for growth of complex materials that include features such as narrow quantum wells or arrays of identical nanowires. We can explain the differences between regimes by considering the asymmetry in the pathways by which the two species arrive at the growth front. We expect our conclusions to apply to other III-V nanowire materials such as GaAs, InAs, and InP. The assumptions underlying the model (surface diffusion, evaporation, and solubility in Au) are common for a range of V and III species. In addition, the crystal structure and defect formation in all four materials are affected in the same way by V/III

ratio (30), suggesting that the effects controlling crystal structure must be general.

#### References and Notes

- P. Caroff *et al.*, *Nanotechnology* **20**, 495606 (2009).
- M. T. Björk *et al.*, *Nano Lett.* **2**, 87–89 (2002).
- J. Johansson, J. Bolinsson, M. Ek, P. Caroff, K. A. Dick, *ACS Nano* **6**, 6142–6149 (2012).
- P. Caroff *et al.*, *Nat. Nanotechnol.* **4**, 50–55 (2009).
- R. E. Algra *et al.*, *Nature* **456**, 369–372 (2008).
- S. Hofmann *et al.*, *Nat. Mater.* **7**, 372–375 (2008).
- C.-Y. Wen *et al.*, *Science* **326**, 1247–1250 (2009).
- F. Glas, J.-C. Harmand, G. Patriarche, *Phys. Rev. Lett.* **104**, 135501 (2010).
- F. M. Ross, *Rep. Prog. Phys.* **73**, 114501 (2010).
- R. E. Diaz, R. Sharma, K. Jarvis, Q. Zhang, S. Mahajan, *J. Cryst. Growth* **341**, 1–6 (2012).
- C.-Y. Wen *et al.*, *Phys. Rev. Lett.* **107**, 025503 (2011).
- K. A. Dick *et al.*, *Nano Lett.* **7**, 1817–1822 (2007).
- K. A. Dick, K. Deppert, T. Mårtensson, W. Seifert, L. Samuelson, *J. Cryst. Growth* **272**, 131–137 (2004).
- J. Johansson, C. P. T. Svensson, T. Mårtensson, L. Samuelson, W. Seifert, *J. Phys. Chem. B* **109**, 13567–13571 (2005).
- R. E. Algra *et al.*, *Nano Lett.* **10**, 2349–2356 (2010).
- J. P. Boulanger, R. R. Lapierre, *Semicond. Sci. Technol.* **27**, 035002 (2012).
- J. P. Boulanger, R. R. Lapierre, *J. Cryst. Growth* **332**, 21–26 (2011).
- F. Jabeen, G. Patriarche, F. Glas, J.-C. Harmand, *J. Cryst. Growth* **323**, 293–296 (2011).
- J. P. Boulanger, thesis, McMaster University (2013).
- Q. Zhang, K. Tateno, T. Sogawa, H. Nakano, *J. Appl. Phys.* **103**, 014301 (2008).
- J. Johansson *et al.*, *Nat. Mater.* **5**, 574–580 (2006).
- M. A. Verheijen, G. Immink, T. de Smet, M. T. Borgström, E. P. A. M. Bakkers, *J. Am. Chem. Soc.* **128**, 1353–1359 (2006).
- H. J. Joyce, J. Wong-Leung, Q. Gao, H. H. Tan, C. Jagadish, *Nano Lett.* **10**, 908–915 (2010).
- P. Krogstrup *et al.*, *J. Phys. D* **46**, 313001 (2013).
- V. G. Dubrovskii *et al.*, *Phys. Rev. B* **79**, 205316 (2009).
- C. Colombo, D. Spirkoska, M. Frimmer, G. Abstreiter, A. Fontcuberta i Morral, *Phys. Rev. B* **77**, 155326 (2008).
- One might expect a logarithmic dependence on  $\nu_V$ , but this dependence is cancelled by the effect of  $\nu_V$  on the group III supply.
- K. W. Schwarz, J. Tersoff, *Nano Lett.* **11**, 316–320 (2011).
- Because the twinning exchanges A and B planes, inclined sidewalls allow the cross section to change gradually to a trigonal hexagon in which wide and narrow sidewalls are also exchanged.
- S. Lehmann, J. Wallentin, D. Jacobsson, K. Deppert, K. A. Dick, *Nano Lett.* **13**, 4099–4105 (2013).

**Acknowledgments:** Supported by the Center for Functional Nanomaterials, Brookhaven National Laboratory, which is supported by the U.S. Department of Energy, Office of Basic Energy Sciences, under contract DE-AC02-98CH10886 (Y.-C.C.); NSF grant DMR-0907483; and the Nanometer Structure Consortium at Lund University, the Swedish Research Council, the Swedish Foundation for Strategic Research, and the Knut and Alice Wallenberg Foundation. Y.-C.C. and K.H. performed experiments and data analysis, J.T. developed the growth model, M.C.R. developed the experimental techniques, and K.A.D. and F.M.R. designed the experiments and coordinated the analysis.

#### Supplementary Materials

www.sciencemag.org/content/343/6168/281/suppl/DC1  
Supplementary Text  
Figs. S1 and S2  
Movies S1 and S2  
References (31–35)

13 August 2013; accepted 11 December 2013  
10.1126/science.1244623

## Temporal Constraints on Hydrate-Controlled Methane Seepage off Svalbard

C. Berndt,<sup>1\*</sup> T. Feseker,<sup>2</sup> T. Treude,<sup>1</sup> S. Krastel,<sup>1†</sup> V. Liebetrau,<sup>1</sup> H. Niemann,<sup>3</sup> V. J. Bertics,<sup>1‡</sup> I. Dumke,<sup>1</sup> K. Dünbnier,<sup>1§</sup> B. Ferré,<sup>4</sup> C. Graves,<sup>5</sup> F. Gross,<sup>1</sup> K. Hissmann,<sup>1</sup> V. Hühnerbach,<sup>5||</sup> S. Krause,<sup>1</sup> K. Lieser,<sup>1</sup> J. Schauer,<sup>1</sup> L. Steinle<sup>3</sup>

Methane hydrate is an icelike substance that is stable at high pressure and low temperature in continental margin sediments. Since the discovery of a large number of gas flares at the landward termination of the gas hydrate stability zone off Svalbard, there has been concern that warming bottom waters have started to dissociate large amounts of gas hydrate and that the resulting methane release may possibly accelerate global warming. Here, we corroborate that hydrates play a role in the observed seepage of gas, but we present evidence that seepage off Svalbard has been ongoing for at least 3000 years and that seasonal fluctuations of 1° to 2°C in the bottom-water temperature cause periodic gas hydrate formation and dissociation, which focus seepage at the observed sites.

Large quantities of methane, a powerful greenhouse gas, are present in the continental margin west off Svalbard, where they are stored as marine gas hydrate (1–3). Because hydrate stability is temperature-dependent, Arctic warming is a potentially major threat to both the environment and the global economy. If even a fraction of the methane contained in Arctic hydrates were released to the atmosphere, the effect on climate could be dramatic (4, 5).

Water-column temperature measurements and mooring data suggest a 1°C bottom-water temperature warming for the past 30 years (6, 7). Numerical modeling of hydrate stability predicts that such warming would result in the dissociation of hydrates in the shallowest sediments (6–9). Therefore, the discovery of numerous gas flares—that is, trains of gas bubbles in the water column precisely at the water depth where gas hydrate is expected to dissociate—was interpreted as the

onset of submarine Arctic gas hydrate dissociation in response to global warming, which may potentially lead to large-scale escape of methane into the water column and ultimately into the atmosphere (6). In order to assess the consequences of methane venting on ocean and atmosphere composition, it is necessary to establish how the rates of methane emissions from hydrate systems change through time (10).

The margin of Svalbard (Fig. 1) can be considered a model system to study a temperature-related gas hydrate destabilization scenario, because water temperature in the Fram Strait oceanographic gateway will be more affected by changes in global atmospheric temperature than elsewhere in the Arctic; therefore, any corresponding changes to a hydrate system should be

<sup>1</sup>GEOMAR Helmholtz Centre for Ocean Research Kiel, 24148 Kiel, Germany. <sup>2</sup>MARUM Center for Marine Environmental Sciences and Faculty of Geosciences, University of Bremen, 28359 Bremen, Germany. <sup>3</sup>Department of Environmental Sciences, University of Basel, 4056 Basel, Switzerland. <sup>4</sup>CAGE (Centre for Arctic Gas Hydrate, Environment, and Climate), Department of Geology, University of Tromsø, 9037 Tromsø, Norway. <sup>5</sup>National Oceanography Centre, Southampton SO14 3ZH, UK.

\*Corresponding author. E-mail: cberndt@geomar.de

†Present address: Institute of Geosciences, University of Kiel, 24118 Kiel, Germany.

‡Deceased.

§Present address: Institut für Angewandte Geowissenschaften, Technische Universität Berlin, 10587 Berlin, Germany.

||Present address: GEOMAR Helmholtz Centre for Ocean Research Kiel, 24148 Kiel, Germany.